Inelastic scattering of pions by ^{10}B

B. Zeidman and D. F. Geesaman
Physics Division, Argonne National Laboratory, Argonne, Illinois 60439

P. Zupranski* and R. E. Segel
Northwestern University, Evanston, Illinois 60201

G. C. Morrison
Birmingham University, Birmingham, England

C. Olmer
Indiana University, Bloomington, Indiana 47405

G. R. Burleson and S. J. Greene†
New Mexico State University, Las Cruces, New Mexico 88003

R. L. Boudrie and C. L. Morris
Los Alamos National Laboratory, Los Alamos, New Mexico 87545

L. W. Swenson
Oregon State University, Corvallis, Oregon 97331

G. S. Blanpied and B. G. Ritchie‡
University of South Carolina, Columbia, South Carolina 29208

C. L. Harvey Johnstone§
University of Texas, Austin, Texas 78712
(Received 5 April 1988)

The inelastic scattering of 162-MeV pions was studied over the angular range 35° to 100° in the laboratory system and the data were analyzed with a model that incorporates shell-model wave functions into a distorted-wave impulse approximation formalism. Reduced transition probabilities were obtained for low-lying levels and compared with information previously reported. In addition, evidence is obtained for theoretically predicted levels with high spin that have not been observed previously.

I. INTRODUCTION

Although ^{10}B has been studied extensively, both experimentally and theoretically, for many years, detailed information[1] exists only for the low-lying levels. Shell-model wave functions[2] provide good descriptions of transitions to, from, and between bound states that are treated in terms of $1p$-shell nucleons outside a closed $1s$-core. Negative parity states which arise from excitations of nucleons into the $2s$-$1d$ shell are poorly understood. In addition, the density of states at excitation energies greater than approximately 6 MeV makes unambiguous identification of levels difficult, particularly when comparing data obtained with different probes. Moreover, the analysis of the inelastic scattering of nucleons and ^3He have utilized collective models that are not suitable for the magnetic transitions observed in electron scattering.

The present study involves the inelastic scattering of pions with kinetic energies of 162 MeV, i.e., near the (3,3) resonance. In this energy regime, distinctive angular distributions are observed and the magnitudes of the cross sections may be related to microscopic descriptions of the wave functions. The present data provide a consistent study of both the well-understood low-lying levels and excitations involving promotion of nucleons into the $2s$-$1d$ shell. It is therefore possible, for the first time, to compare results for hadronic scattering in ^{10}B with data for electron scattering and also to infer the excitation of high spin states that have not been reported previously.

II. EXPERIMENTAL PROCEDURES

The experiment was performed with the use of the EPICS system[3] at LAMPF. The mean energy of the incident pion beams was 162.5 MeV. Positive pion spectra were obtained at scattering angles from 20° to 100° in 5° steps, except for 95°. Shorter negative pion runs were taken over the angular range 20° to 90° to measure elastic scattering cross sections, although longer runs were made

at 10° intervals between 40° and 90° for comparison with the π^+ data.

The ^{10}B target was prepared from isotopically enriched boron powder (92% ^{10}B) that was compressed and sintered to form a plate 100 mg/cm^2 thick. A similar enriched ^{11}B target, 110 mg/cm^2 thick, was also bombarded at each of the angles studied. After subtraction of the ^{11}B contributions, ^{10}B spectra, such as that shown in Fig. 1, were obtained. The relative normalizations of the data were provided by measuring the flux in two ion chambers situated downstream of the target, while the absolute normalization was provided by comparison with scattering from hydrogen, the hydrogen cross sections being obtained from published phase shifts.[4] The uncertainty in the absolute cross sections is estimated to be about ±10% and relative cross sections are believed to be determined to ±5%. Peak areas were extracted from the spectra with the use of a fitting routine in which the line shape was obtained from the elastic peak so as to insure that yields were extracted in a consistent fashion. The overall resolution for low-lying states was ~220 keV [full-width at half-maximum (FWHM)], but may be larger at high excitation energies as intrinsic widths increase.

Since ^{10}B is a light, $T=0$ target, it was expected, and verified, that similar cross sections would be obtained in π^+ and π^- scattering. Indeed this is the case for elastic scattering as is seen in Fig. 2. Since no significant differences between π^+ and π^- cross sections were observed in the present experiment, data from both polarities were combined in the analysis of the angular distribution data.

III. DATA ANALYSIS AND RESULTS

The procedures used for data analysis were developed by Lee and Kurath[5,6] and have been discussed previously[7] in the analysis of pion scattering on ^{14}N. Shell model wave functions are incorporated into a distorted-wave

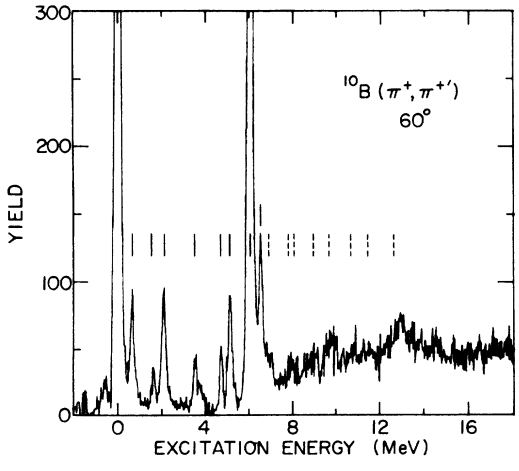

FIG. 1. Spectrum of ^{10}B(π^+,π^+) at 60°. The vertical lines indicate the positions of levels discussed in the text. The solid lines correspond to known, resolved levels while the dashed lines indicate peaks of less certain identification.

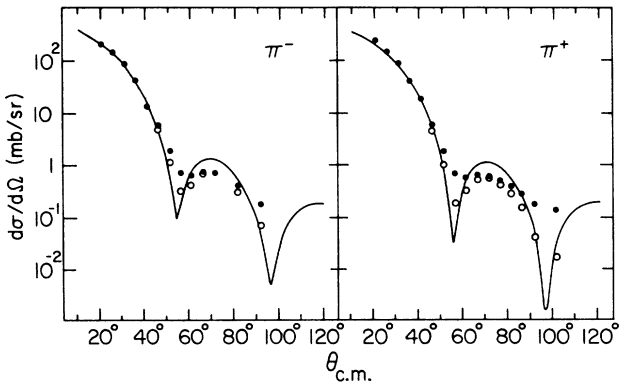

FIG. 2. Elastic scattering of π^- and π^+ by ^{10}B at an incident energy of 162.5 MeV. The curves are PIPIT calculations discussed in the text. The solid points are the measured data while the open circles result from subtraction of quadrupole contributions based upon the measured cross sections for the 6.028 MeV state.

impulse approximation formulated in momentum space. Within this framework positive parity states in ^{10}B arise from $(1p)^6$ configurations, while negative parity states result from particle-hole excitations of the form $(1p)^5(2s,1d)^1$. For the $(1p)^6$ configurations, the calculations utilize Cohen-Kurath wave functions,[2] while modified Millener-Kurath wave functions[8] are used for the particle-hole excitations. The transition amplitudes in the distorted-wave impulse approximation (DWIA) are composed of two primary constituents, namely the nuclear transition densities and the pion-nucleus distorted waves derived from elastic scattering. When the transition amplitudes are expressed in a $J(LS)$ representation, each $J(LS)$ term, i.e., multipole, leads to a distinctive angular distribution shape whose magnitude is weighted by the appropriate transition density. Generally, strong transitions are dominated by a single multipole, but the large spin of ^{10}B allows more than one multipole to contribute to the transition to a given state, the overall angular distribution being composed of the incoherent sum of terms from each J multipole. More complete discussions of the formalism, including representative differential cross sections for the various multipoles have been presented previously.[6,9]

In the absence of isospin mixing, the formalism implies particularly simple relationships for $T=0$ targets such as ^{10}B. For pion scattering near the (3,3) resonance the differential cross section may be written as

$$\frac{d\sigma}{dw}(\theta)=\left[\frac{2J_f+1}{2J_i+1}\right]\{A_p[3+(-1)^T]\}^2 C_{Jls}(\theta)$$

where $J_i(J_f)$ is the spin of the initial (final) state of the target, C_{Jls} is the appropriate differential cross section from the DWIA and A_p is the one-body transition density. The assumption of delta dominance is reflected in the term $[3+(-1)^T]$, where T is the isospin of the final state.

The reduced transition probabilities, $B(EJ)$ and

$B(MJ)$, may be written in the form

$$B(\xi J)=\left[\frac{2J_f+1}{2J_i+1}\right]\{A_p[\nu_p+(-1)^T\nu_n]\}^2 N_{Jls}$$

where ξ is E or M, and $\nu_p(\nu_n)$ is either the effective charge, $e_p(e_n)$ for electric transitions or $\mu_p(\mu_n)$, the nucleon magnetic moment, for magnetic multipoles. N_{Jls} is the normalization constant for each multipole. For collective excitations that are not adequately described within the $1p$-shell model space, it has been shown[5] that agreement with measured electromagnetic transition probabilities may be obtained through the use of either effective charges or enhanced transition densities. Inasmuch as single particle transitions imply free nucleon values, i.e., $e_p=1$, $e_n=0$, these values will be assumed for all subsequent discussion and enhancement, if any, will be attributed to the transition density. Since both the differential cross section and the reduced transition probability depend upon the common factor,

$$\left[\frac{2J_f+1}{2J_i+1}\right](A_p)^2 ,$$

it is seen that a reduced transition probability may be obtained directly from the experimental results despite ignorance of both the spin of the final state and detailed knowledge of the transition density. For a given cross section, however, the extracted value of $B(\xi J)$ will be four times greater for an electric transition, and 114 times greater for a magnetic multipole if the isospin of the final state is 1 rather than 0.

A. Elastic scattering

The angular distributions for elastic scattering of both π^+ and π^- are shown in Fig. 2 together with curves obtained from calculations performed with the program PIPIT.[10] The range parameter, b, used for the Gaussian ground-state density was taken to be 1.40 fm. No adjustment to parameters was undertaken inasmuch as consistency with the nuclear structure calculations was desired.

The defects in these calculations, although quite apparent, are relatively unimportant for the subsequent analysis. The primary result of the calculations is the proper choice of nuclear radius, evident in the good agreement at forward angles. If a slightly different density distribution had been chosen, such that the effective diffuseness at the nuclear surface was larger, the secondary maximum in the calculations would have been reduced to agree with the data.

The absence of a well defined minimum is a reflection of the elastic quadrupole scattering previously discussed in $\pi-{}^9$Be scattering.[11] Indeed, the larger quadrupole moment of ^{10}B suggests that the minima in the elastic scattering angular distributions should be filled in even more for ^{10}B than for ^{9}Be, as is the experimental observation. The open circles shown in Fig. 2 result from subtraction of quadrupole contributions that are obtained from the cross sections for the $E2$ transition to the collective state at 6.028-MeV excitation; the improved agreement with the calculated curve is apparent.

For inelastic scattering, the shapes of the calculated angular distributions are, in principle, derived from the "fit" to the monopole term in the elastic scattering, i.e., the pion-nucleus distorted waves that result, for example, from the PIPIT calculations. It is therefore expected that the calculated angular distributions for inelastic transitions will also tend to overpredict cross sections at secondary maxima.

B. Inelastic scattering to low-lying levels

The angular distributions for transitions to the low-lying positive parity states are shown in Fig. 3 together with theoretical calculations which utilize transition densities that have been published previously.[5] The curves do not involve any fitting or adjustment in magnitude except as specifically noted below. A summary of the results of the analysis is presented in Table I where the multipolarities and reduced transition probabilities deduced from the present data are compared to both theoretical predictions and previous studies with other probes.

In Fig. 3, the angular distributions for the 1^+ states at excitation energies of 0.72 and 2.15 MeV show two curves, as does that for the 2^+ state at 3.59 MeV. The solid curves result from the shell model transition densities for the individual states, while the dashed curves involve a linear combination of the wave functions for the

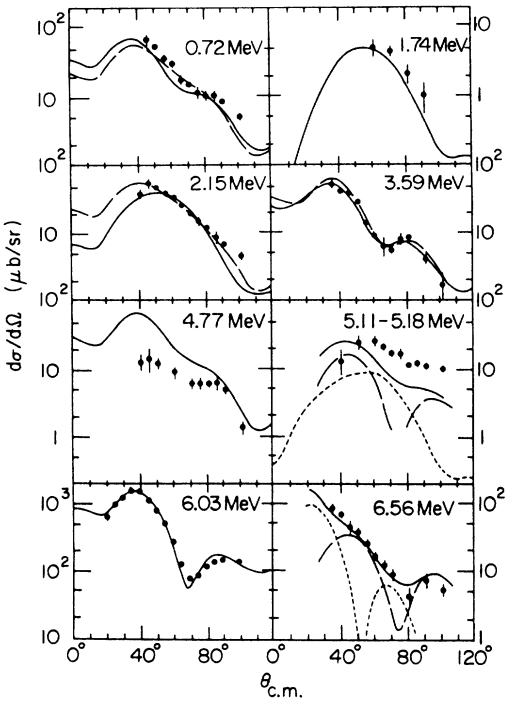

FIG. 3. Angular distributions for inelastic pion scattering to the levels indicated. The various curves are DWIA calculations discussed in the text.

TABLE I. Excitation energies, multipolarities, and reduced transition probabilities for inelastic scattering on ^{10}B. The levels at excitation energies less than 7 MeV have been assigned previously (Ref. 1) as have all indicated spins and parities. The multipole assignments are from the present data. The $B(E\Lambda)$ for the hadronic scattering were calculated from published deformation parameters using the relationship $B(E\Lambda)=(3Z/4\pi)^2R^{2\Lambda}[(2J_f+1)/(2J_i+1)(2\Lambda+1)]\beta^2$, with $\langle R^2\rangle^{1/2}=2.64$ fm. Parts, or all, of the symbol $(J^\pi;T)$ are included in the values of $B(\Lambda)$ to specify the spin and/or isospin for which the value was obtained.

				$B(\Lambda\uparrow)(e^2\text{fm}^{2\Lambda})$			
					Hadronic		
Level	$J^\pi;T$	Multipole	Present data	Electromagnetic	Ref. 13	Ref. 16	Theory
0.72	$1^+;0$	$E2$	$E2=0.92\pm0.15$	1.7	2.7±0.3	0.82±0.2	0.83[0.56][a]
		$+M3$	M3=0.42±0.16				0.15[0.42]
1.74	$0^+;1$	$M3$	$M3=9.5\pm0.12$	6±1.4			8.47
2.15	$1^+;0$	$E2$	$E2=0.46\pm0.12$		1.45±0.25	0.8±0.2	0.16[0.43][a]
		$+M3$	$M3=0.43\pm0.12$				0.56[0.29]
3.59	$2^+;0$	$E2$	$E2=0.67\pm0.10$		2.0±0.3	1.3±0.3	0.53[0.76][a]
4.77	$3^+;0$						$B(E2)=0.68$
5.11[b]	$2^-;0$[b]	$E3$	$E3<10.4$		10.4±2.5		1.6
5.16	$2^+;1$	$M3$	$M3<28$	21.6±2.2			14.3
5.18	$1^+;0$						
6.03[b]	$4^+;0$[b]	$E2$	$E2=20.4\pm2.0$	21.2±1.0	16.3±1.4	7.0±0.7	$5.4\times4=21.6$
6.13	$3^-;0$	$E3$			23.5±2.4		10.2
6.56	$4^-;0$	$E3$	$E3=17.1\pm2.0$		19±3.5	34.5[18]	16.3;$M4=3.5$
		$+E1$	$E1=(4\pm2)\times10^{-3}$				$E1=0$
7.0	$(1^-);0+1$	$M2$	$M2=(1.3\pm0.4)\times10^{-3}(;0)$				3×10^{-4}
	$1^+;0+1$	$+M4$	$M4=0.7\pm0.2$				$3.9\times10^{-2}(T=0)$
7.8	$(1^+;0)$	$E2$	$E2=0.34\pm0.03(;0)$				$0.97(1^+;1);0.12(3^+;0)$
8.07	2^+	$E2$	$E2=3.2\pm0.4(;1)$	4.9±0.5			$1.2(2^+;1)$
8.9	$2^+;3^-;1$	$E3$	$E3=21.7\pm2.0(;0)$	$M2=1.5\pm0.2$, $M3=4.3\pm0.4$, $M1=2.9\pm1\times10^{-4}$			$E3=21.4;M4=3.3(5^-;0)$
9.7	1	$E3$	$E3=9.3\pm3(;0)$				$9.7(3^-;0)$
		$+M3$	$M3=15.1\pm0.5(;1)$				$4.5(2^+;1)$
10.7		$E3$	$E3=9.7\pm2(;0)$				$13.5(4^-;0);5.3(6^-;0)$
	$(2,3,4^+)$	$M1$	$M1=(4.3\pm1.)\times10^{-2}(;1)$	$M1,E2$			$M1=5.3\times10^{-2}(3^+;1)$
11.5		$E2$	$E2=1.4\pm0.4(;1)$				$1.2(4^+;1);0.5(2^+;1)$
		$+M1$	$(5.3\pm1.7)\times10^{-2}(;1)$	$M1=(5.3\pm1.1)\times10^{-2}$			$7.1\times10^{-2}(2^+;1)$
12.8		$M2$	$M2=(1.4\pm0.3)\times10^{-2}(;0)$				$3.7\times10^{-3}(4^-;0)$
		or $E3$	$E3=20\pm10(;0)$				$7.8(5^-;0)$

[a]Admixed wave functions.
[b]Unresolved states.

two lowest states of each spin. The admixture of 16% follows from analysis of gamma decay.[12]

The peak at approximately 5.15 MeV excitation consists of unresolved contributions from the $2^-;0$ state at 5.11 MeV, the $2^+;1$ state at 5.17 MeV, and a $1^+;0$ state at 5.18 MeV. The dashed curve in Fig. 3 is the predicted contribution from the $2^+;1$ state, while the long-dashed curve is the $E3$ strength for the 2^- state that is derived from a study of proton inelastic scattering[13] on ^{10}B. Inasmuch as the 1^+ state is theoretically believed to involve a two-particle excitation, it was assumed that the 1^+ state does not contribute to the peak.

The 2^+ state at an excitation energy of 5.92 MeV is obscured since the transition to the 4^+ state at 6.03 MeV excitation, the only known member of the rotational band built upon the 3^+ ground state, dominates the spectrum shown in Fig. 1. The angular distribution exhibits a definite $E2$ shape whose magnitude is enhanced, as predicted,[5] over the shell model value. Moreover, the angular distribution for the 2^+ state is also predicted to exhibit an $E2$ shape, so that there is no angular dependence to aid separation.

C. Transitions to unbound states

While there are many known states of ^{10}B at higher excitation energies, there is little definitive information available. As a result, the curves shown in Fig. 4 result from a subjective fitting procedure involving the incoherent addition of contributions from various multipoles. These results are also presented in the table. In many cases, the deduced multipolarities might have been constrained by known spins and parities, but given both the statistical uncertainties in the data as well as the high density of states, there is no assurance that the observed peaks result from previously assigned levels or even single states. This is particularly true when the decomposition suggests assignments with opposite parities. In addition, many of the previous assignments have been made on the basis of compound nuclear analyses or nucleon transfer

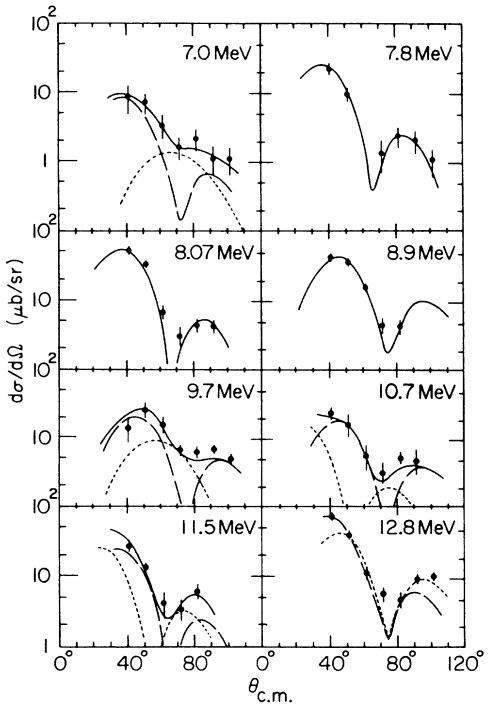

FIG. 4. Angular distributions for pion inelastic scattering to peaks at the excitation energies as indicated in the figure. When more than one DWIA curve is shown, the solid curve is the sum of the other curves, except for the 12.8 MeV peak for which no sum is shown.

reactions. Since the spin of ^{10}B is 3^+, and the adjacent nuclei have spins of $\frac{3}{2}$ or less, it is extremely unlikely that states with spins greater than three or four would have been observed with the intensities required for assignment.

IV. DISCUSSION OF RESULTS

Since there is usually a high degree of selectivity involved in reactions that are induced by different probes, relatively few studies of ^{10}B allow direct comparison between data for electric and magnetic transitions that may be obtained in either strong interactions or electromagnetic interactions. As indicated in the previous section, for a given transition probability, isoscalar transitions are favored in pion scattering, and moreover, when $B(\xi\Lambda)$ is expressed in units of $e^2\text{fm}^{2\Lambda}$ rather than $\mu_N^2\text{fm}^{2\Lambda-2}$, magnetic transitions have much smaller $B(\Lambda)$ values than the corresponding electric multipoles. The summary presented in Table I provides a comparison of the present results with theoretical predictions[5,15] and previous data. However, in order to obtain $B(E\Lambda)$ values from the collective model employed in the analysis of previous hadronic interactions, it is necessary to assume a value for an effective interaction radius. The radius used for the comparison is consistent with that used for both the shell model calculations and the optical model calculations, but is not necessarily optimal for the proton[13] and ^{3}He scattering.[16] Since $B(E\Lambda)$ varies as $R^{2\Lambda}$, small changes in R can result in large changes in the values of $B(E\Lambda)$ derived from the measured deformation parameters. In contrast, the present analysis, electromagnetic interactions, and the shell model calculations are treated on a similar basis, have no explicit radius parameter dependence, and should be directly comparable.

Pion scattering to the 1^+ states at 0.72- and 2.15-MeV excitation proceeds primarily via $E2$ excitation, both theoretically and experimentally, although there is also a noticeable $M3$ component. Admixing the shell model wave functions[12,14] produces the significant improvement in the shapes of the angular distributions shown in Fig. 3 and reasonably good agreement for the cross sections. The present $B(E2)$ value for the 0.72-MeV state is larger than either theoretical prediction, although smaller than that obtained from the measured lifetime of the state, while that of the 2.15-MeV level is close to the mixed value. The deformation parameters, β, extracted from ^{3}He scattering[16] result in $B(E2)$ values similar to the present one for the 0.72-MeV level and larger for the 2.15-MeV state. For both states, the $B(E2)$ values from proton scattering[13] are considerably larger.

The transition to the 2^+ state at 3.59 MeV excitation is in reasonable agreement with the theoretical predictions, both with and without admixtures. Since the shell model wave function for the unresolved, second 2^+ state at 5.92 MeV contains a qualitatively similar multipole mixture, little change in shape or magnitude is expected to result from admixture. Again the reduced transition probabilities derived from the collective model are much larger than the present results.

In contrast to the agreement observed for the lower states, there is a complete lack of agreement in both shape and magnitude for the 3^+ state at 4.77 MeV excitation. Indeed, the angular distribution is not amenable to a reasonable decomposition into multipole contributions. There appears to be a significant $E2$ component that would be about $\frac{1}{5}$ the predicted strength, but the residual angular distribution is not even suggestive of any multipolarity. Previous inelastic scattering studies have also been unable to provide multipole assignments.

The most prominent feature observed in the present data is the peak corresponding to the 4^+ state at 6.028-MeV excitation whose $B(E2)$ is about four times the unenhanced predicted value. The $B(E2)$ value obtained in the present study is consistent not only with those obtained in electromagnetic interactions,[17] but also with those derived from deformation lengths, βR, measured in the inelastic scattering of protons and heavier nuclei. The enhancement of this rotational $E2$ transition is consistent with that obtained for other collective $E2$ transitions in this mass range where the effective transition amplitude, or effective charge, is roughly twice that arising from purely $1p$-shell or spherical configurations.

In the collective model, which is particularly appropriate for this rotational state, the $B(E2)$ for a transition to a rotational state is directly related to the intrinsic electric quadrupole moment of the nucleus and the quadrupole component of elastic scattering. With this assumption, the $B(E2)$ for the 4^+ state implies a ground-state electric quadrupole moment of 89 ± 5 mb, which is in

surprisingly good agreement with the measured value, ~ 85 mb. These values imply an enhancement factor of ~ 1.8 for the $E2$ transition amplitude of the ground state relative to the theoretical prediction;[5] an enhancement factor of 1.95 is required for the 6.028 MeV state.

The 6.13-MeV, $3^-;0$ level is not resolved in the present study, although it may contribute to the peak attributed to the 4^+ state. Because of the angular distribution difference, however, an $E3$ transition of either the predicted strength or that measured in proton scattering would still result in contributions to the differential cross section so small compared to those of the collective transition as to be unmeasurable.

The excitations of the $T=1$ states at 1.74 MeV, O^+, and 5.16 MeV, 2^+, involve primarily $M3$ transitions. The magnitude of the cross section for the 0^+ state is consistent with the theoretical prediction, the curve shown in Fig. 3, but somewhat better agreement is obtained with a $B(M3)$ about 15% greater. In Table I we see that the value reported for inelastic scattering of electrons,[17] however, is slightly smaller.

As noted earlier, the transition to the 5.16-MeV state is unresolved and a clear decomposition of the angular distribution is hindered by the poor data at the more forward angles. It appears that an angular distribution calculated from a combination of the theoretical prediction and an $E3$ contribution has the correct shape for angles greater than $\sim 60°$, although too low a cross section. Since the curve displayed in Fig. 3 already exceeds the data at the most forward angle, it is not possible to renormalize the curves to fit the data. If the two forward angle points were ignored, however, the $B(M3)$ so obtained would be in excellent agreement with the electron scattering result and the β value for the $E3$ component obtained from proton scattering. Such a large value for $B(E3)$ implies significant enhancement and suggests collective $E3$ excitation.

The angular distribution of the state at an excitation energy of 6.56 MeV is rather unusual not only in the present study, but also in other work.[16] The state most probably has $J^\pi=4^-$, $T=0$ and corresponds to the yrast 4^- state in the shell model calculations. Previous nucleon scattering studies[13,18] have identified $E3$ contributions, but the angular distributions are not fitted well by the calculated curves. In the present case, shown in Fig. 3, it would be difficult to justify an $E3$ assignment for the transition without significant admixture of another multipole. Indeed, the $E3$ strength extracted from the data is in reasonable agreement with both the previous results and theoretical predictions for the yrast 4^- state. The residual yield, however, is unambiguously consistent only with an $E1$ contribution, which is forbidden in the absence of recoil. The deduced strength of 0.04 Weisskopf units for the $E1$ is much greater than can be expected for transitions between $T=0$ states when recoil is considered.

A number of additional peaks were observed in the spectra at excitation energies corresponding to states previously identified. The excitation energies and multipole decompositions are tabulated along with the previous identification. In some instances, the peaks may also be

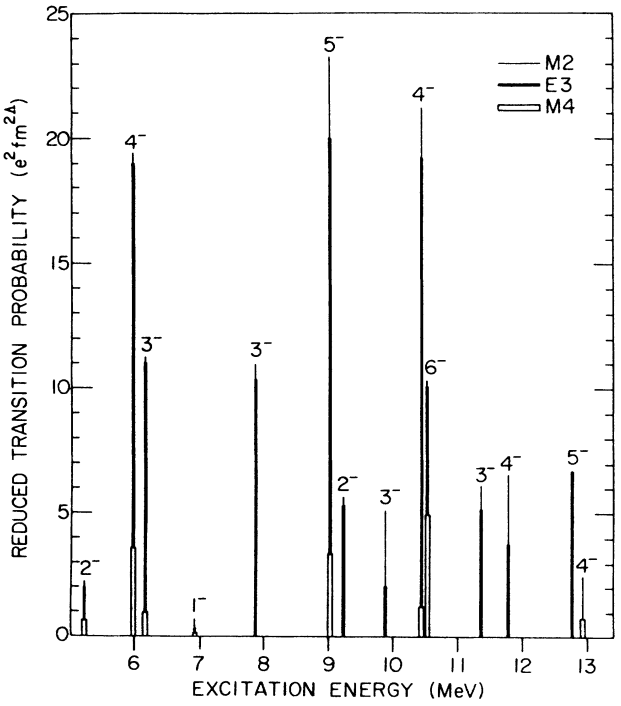

FIG. 5. Theoretical excitation energies, spins and $B(\xi\Lambda)$ for strong negative parity transitions. The reduced transition probabilities for $M2$, $E3$, and $M4$ are denoted by increasing widths of the vertical bars; the $B(M2)$ values are multiplied by 10^3.

correlated with states predicted[15] by the shell model calculations. Shown in Fig. 5 are the expected excitation energies and $B(\xi J)$ for strong negative parity transitions. The peak positions have been shifted empirically by $(0.25-0.4J_f)$ MeV relative to the theoretically calculated excitation energies so as to provide somewhat better agreement for the previously identified levels. In the complete spectrum there are many additional weaker levels, but these are not expected to have cross sections that are observable above background. Given uncertainties in the energy scale, ~ 100 keV, coupled with the high density of states, however, it is not certain that the observed peaks correspond to the states previously noted or even that the peaks involve excitation of individual levels.

For example, the angular distribution for the peak at an excitation energy of 7.0 MeV appears to have an $M2+M4$ multipole decomposition, so that negative parity is favored. The previously identified peak at 7.0 MeV was assigned positive parity, although a $1^-, T=0+1$, state was assigned[1] at 6.873 MeV excitation. Inasmuch as the excitation energy scale is established by the nearby state at 6.56 MeV, it would be difficult to conclude that the peak corresponds to either of the two previously observed levels. A similar problem arises with the peak at an excitation energy of 7.8 MeV, for which an $E2$ transition is suggested. Although in this case it is possible to correlate the peak with a tentative 1^+ assignment at 7.67 ± 0.03 MeV, a 1^- state has been identified at 7.81 MeV in the $^9\mathrm{Be}+p$ reaction.

A strong $E2$ transition was observed in electron

scattering[19] to a broad peak at an excitation energy of 8.07 MeV. While the present data confirm an $E2$ excitation at 8.07 MeV, the peak is not particularly broad and, for $T=0$, the $B(E2)$ value is only 15% of that previously obtained. Even if the $E2$ part of the 7.8 MeV peak is added, the total strength would be less than 25% of that reported. It is clear that the previous analysis would be in error unless $T=1$ is assigned to these peaks. As indicated in the table, several $E2$ transitions are predicted in this region of excitation energy, but unless there is enhancement, none would have the observed strength.

At approximately 8.9 MeV excitation, two $T=1$ states that are analogs of 2^+ and 3^- states in ^{10}Be have been reported. Although both an $M2$ and an $M1$, $M3$ admixture have been assigned previously,[17] the present data suggest an $E3$ assignment which is consistent with population of a 3^- state. The 3^- state has also been observed in neutron scattering by ^{9}Be and in the ^{9}Be$(d,p)^{10}$ Be reaction[1] with angular momentum transfer, $l=2$. Since the microscopic description of an $E3$ excitation involves exactly this particle-hole operation, it might be reasonable to assign the peak to excitation of the 3^- state. With the $T=1$ assignment, however, the measured $B(E3)$ is much larger than is predicted. The yrast 5^- state, however, is expected at an excitation energy of roughly 9 MeV with nearly the $B(E3)$ observed, but would not have been observed in the reactions on ^{9}Be. No other state is predicted in this region with a strength comparable to the measured value.

The peak near 9.7 MeV excitation has been seen previously, but no assignment has been made. The present data suggest a mixture of $E3$ and $M3$ transitions which is consistent only with a doublet. The $M3$ component is consistent with a 2^+; 1 state that is predicted in the vicinity. The negative parity states probably involve high spins, since it is anticipated that low spin states would have been identified previously. A 4^-;0 state is expected at an excitation energy of about 10 MeV, as are other 3^- states. The "prediction" in the table should be considered as a tentative suggestion.

The decomposition of the angular distribution for the peak at approximately 10.7 MeV excitation suggests a combination of $M1$ and $E3$ transitions. The $M1$ term agrees with an $M1$ tentatively assigned in (e,e') and positive parity for a 10.8 MeV level. While the negative parity arising from an $E3$ transition is inconsistent with data previously reported for ^{10}B, there is a tentative assignment of 4^- for a state in ^{10}Be at an excitation energy of 9.27 MeV whose analog in ^{10}B would appear at an energy of approximately 10.7 MeV. Several 4^- states, including one with $T\simeq 1$ are predicted near this excitation energy, but only the second 4^-;0 has the requisite strength. On the other hand, several 3^- states and the yrast 6^- state, all with reasonably strong $E3$ components, are expected in this region.

The peak at 11.5 MeV excitation appears in both (e,e') and neutron pickup reactions. The present data suggest $M1+E2$ excitation, consistent with positive parity, and the tentative $M1$ assignment in (e,e') and neutron pickup on ^{11}B. In this region of excitation, it is expected that several 2^+;1 states will be populated by mixed $M1,E2$ transitions.

The peak near 12.7 MeV excitation appears to be a relatively strong $M2$ or $E3$ transition. A broad resonance, unassigned, is seen in ^{9}Be(p,γ) and a peak is observed in (e,e'). $M2$, $E3$ transitions imply negative parity, and a number of negative parity states with both low and high spins are expected at excitation energies around 12.7 MeV. The dearth of supporting information makes even tentative assignments of spin impossible, although some possibilities are indicated in the table.

V. CONCLUSION

The analysis of the inelastic scattering of 162 MeV pions by ^{10}B has been shown to provide transition probabilities for low-lying states that are in good agreement with results for inelastic electron scattering and with theoretical predictions that describe the electromagnetic transitions between excited states. In addition, data have been obtained for unbound states and negative parity states that arise from excitations into the $2s$-$1d$ shell. There is good qualitative agreement between the present results and shell model calculations that extend beyond a simple $1p$-shell model space. The present study, together with other recent work, provides clear evidence that pion inelastic scattering is a reliable tool for detailed investigations of nuclear structure and may be particularly useful in providing new information complementary to that obtained with other, more restricted, electromagnetic and strongly interacting probes. High spin states that are inaccessible or obscured in transfer reactions, compound nuclear studies, or electron scattering are readily observed in pion inelastic scattering. In particular the $E3$ strength measured at excitation energies near 10 MeV in ^{10}B may be evidence for transitions to 5^- and 6^- levels. The present data, while not conclusive, provide a basis for further investigation of highly excited, high spin states that may be populated in cluster transfer in heavy ion reactions.

ACKNOWLEDGMENTS

We thank Dr. Dieter Kurath for his invaluable assistance which included numerous discussions and unpublished calculations. Particular thanks are due F. Karasek who fabricated the Boron targets. We would also like to thank the staff and management of LAMPF for their cooperation and assistance. This work supported by the Department of Energy, Nuclear Physics Division, under Contracts W-31-109-ENG-38 and DE-AS04-76ER03591, and the National Science Foundation.

*Permanent address: Institute for Nuclear Research, Warsaw, Poland.
†Present address: Los Alamos National Laboratory, Los Alamos, NM 87545.
‡Present address: Arizona State University, Tempe, AZ 85287.
§Present address: Fermi National Laboratory, Batavia, IL 60510.

[1]Fay Azjenberg-Selove, Nucl. Phys. **A413**, 1 (1984).
[2]S. Cohen and D. Kurath, Nucl. Phys. **73**, 1 (1965).
[3]H. A. Thiessen *et al.*, Los Alamos Scientific Laboratory Report, LA-4534MS, 1970.
[4]C. Rowe, M. Solomon, and R. H. Landau, Phys. Rev. C **18**, 584 (1978); Nucl. Phys. **A226**, 213 (1974).
[5]T.-S. H. Lee and D. Kurath, Phys. Rev. C **21**, 293 (1980).
[6]T.-S. H. Lee and D. Kurath, Phys. Rev. C **22**, 1670 (1980).
[7]D. F. Geesaman *et al.*, Phys. Rev. C **27**, 1134 (1983).
[8]D. J. Millener and D. Kurath, Nucl. Phys. **A255**, 315 (1975).
[9]B. Zeidman and D. F. Geesaman, Nucl. Phys. **A396**, 419c (1983).
[10]R. A. Eisenstein and F. Tabakin, Comput. Phys. Commun. **12**, 237 (1976).
[11]D. F. Geesaman *et al.*, Phys. Rev. C **18**, 2223 (1978).
[12]E. K. Warburton *et al.*, Phys. Rev. **171**, 1178 (1968).
[13]R. U. Swiniarski *et al.*, Helv. Phys. Acta **49**, 227 (1976).
[14]D. Kurath, Nucl. Phys. **A317**, 175 (1979); private communication.
[15]D. Kurath, private communication.
[16]G. T. A. Squier *et al.*, Nucl. Phys. **A119**, 369 (1968).
[17]E. J. Ansaldo *et al.*, Nucl. Phys. **A322**, 237 (1979).
[18]B. Vaucher, J. C. Alder and C. Joseph, Helv. Phys. Acta **43**, 237 (1970).
[19]L. W. Fagg *et al.*, Phys. Rev. C **14**, 1727 (1976).